Journal of Thermal Analysis and Calorimetry, Vol. 82 (2005) 179–184

IDENTIFICATION OF MICRO-SCALE CALORIMETRIC DEVICES Part VI. An approach by RC-representative model to improvements in TAM microcalorimeters

R. Kirchner[1], *M. Rodriguez de Rivera*[2], *J. Seidel*[1] *and V. Torra*[3*]

[1]Institute of Physical Chemistry, TU Bergakademie Freiberg, D-09596 Freiberg/Sachsen, Germany
[2]Physics Department, University of Las Palmas, E-35017 Las Palmas de Gran Canaria, Spain
[3]CIRG-DFA-ETSECCPB, Polytechnical University of Catalonia, Campus Nord B4-B5, E-08034 Barcelona, Catalonia

Using an RC model, the behavior of a TAM high-performance calorimeter (Thermometric AB, Sweden) equipped with a flow-mixing insertion vessel using independent pumps for each reactant is studied. The model shows a reliable sensitivity behavior for mixtures realized inside the cell. The model behavior is compared with experimental measurements.

Keywords: *calibration, flow microcalorimeter, liquid mixtures, heat transfer model*

Introduction

The study of enthalpies of mixing requires adapted devices. In fact, when liquids continuously flow through a reaction chamber the sensitivity –Joule or chemical- usually shows a dependence on the flow rate. For instance, using appropriate low flow rates in the 2277-204 device (Thermometric AB with user modified output) the sensitivity changes do not exceed 8% (Fig. 1). The changes are particular for each fluid flow (f_1 and f_2), however, using the volumetric heat capacities for the mixture (the density multiplied by the heat capacity or ρc_p), some similar behavior can be deduced [1, 2]. In a reduced domain around 0.01 in $\rho c_p f$ units (WK^{-1}) the peak to peak maximal fluctuation remains below 3%.

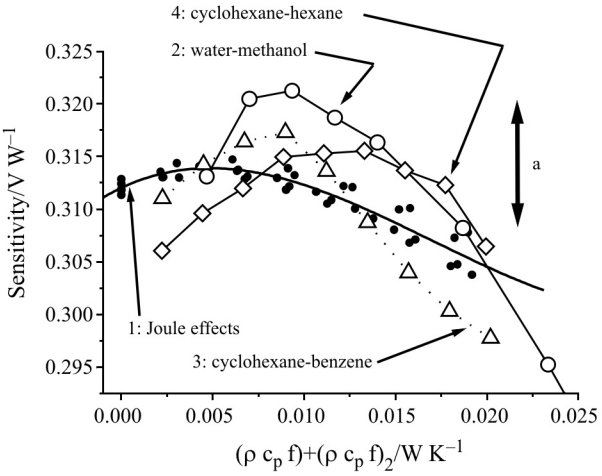

Fig. 1 Sensitivity against the $(\rho c_p f)_{1+(}\rho c_p f)_{2.}$. 1: global fit for Joule effect measurements with injection of water, methanol, benzene, hexane and cyclohexane (black dots); 2, 3 and 4: sensitivity using standard mixtures, water+methanol (2), benzene+cyclohexane (3) and cyclohexane+hexane (4). The arrow a represents a 3% peak to peak interval

In general, the rate dependence of sensitivity can be associated with a varying portion of the dissipated heat flux detected by the thermopiles [3]. Starting from zero, an increase of the flow rates moves the mixing zone towards the detector position (increasing the detected signal) and, for higher flow rates, an increasing part of heat is directly sent to the surroundings without any effect on the detector.

The detection effects associated to partial heat flux integration are one of the old – and always new-problems in conduction calorimeters. In fact, the detection zone is extremely reduced especially for nano-sized calorimeters, i.e., using silicon flat surface [3–6]. These instruments use detectors encircling the two-dimensional working surface (x-y coordinates). For instance, the integrated thermocouples (i.e. Al–Si) in silicon membranes form a 'line' as a detection zone [references?]. Reliable measurements giving an approach to thermodynamic enthalpies require some sophisticated analysis, in particular, when the heat is dissipated above (in the z-coordinate direction) the silicon surface containing the detector. In fact, the main target of this and previous papers I, II, III, IV and V [3–7] is the analysis of flows of heat and matter in 'calorimetric' devices for improved quantitative results.

* Author for correspondence: vtorra@fa.upc.edu

1388–6150/$20.00

Akadémiai Kiadó, Budapest, Hungary
Springer, Dordrecht, The Netherlands

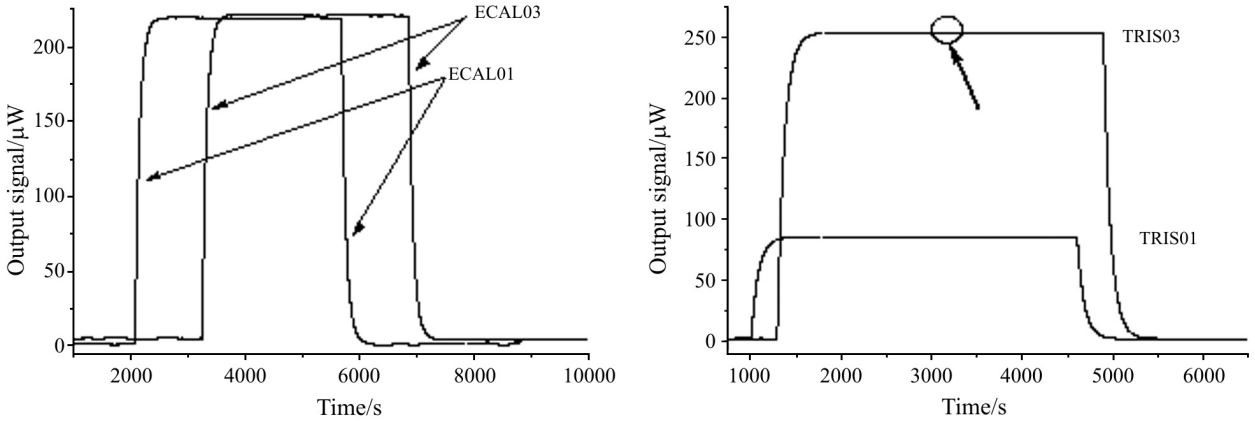

Fig. 2 Joule effect signals (left) and TRIS protonation (right) at 0.2 and 0.6 mL min^{-1} total flow rate. Arrow: enlarged zone (Fig. 3)

In this paper, the behavior of an improved version of the TAM microcalorimeter –heat flow detector and flow-mix insertion vessel- is partially analyzed and a RC model is build. The effects of the dissipation position are simulated using MATLAB tools (http://www.mathworks.com/).

Experimental system

The studied flow microcalorimeter is a TAM instrument (Nanowatt version 2277-012) equipped with an improved heat flow detector structure (4 mL High Performance Ampoule Microcalorimetric Unit 2201) and a new flow vessel (Flow-Mix Insertion Vessel 2250-007, Thermometric, AB). The calorimetric measurement is controlled by the DIGITAM instrument software. All experiments have been carried out at 25°C.

The flow delivery system consists of two computer controlled HPLC-pumps (K-1001, double-piston design, Knauer, Germany). The internal Joule-effect calibration heater (power 249.8 μW, time 3600 s) and the reaction of TRIS (0.1 mol L^{-1}) with hydrochloric acid (1.655 mmol L^{-1}) at different flow rates were used for calibration. The built-in heater for the electrical calibration is located in the calorimetric device (under the bottom of the calorimetric cell). Figure 2 (left) shows the calorimetric output (curve) for two electrical calibration steps (dissipated power 249.8 μW) corresponding to two different total flow rates (0.2 and 0.6 mL min^{-1}). The right side of Fig. 2 shows the calorimetric signals corresponding to the reaction of TRIS with hydrochloric acid at total flow rates of 0.2 and 0.6 mL min^{-1} (a half for each pump), respectively. The time constant of these curves are summarized in Table 1.

Using a sensitivity defined, as usual in control systems, by 'output signal'/'input signal' the values for zero flow, 0.2 and 0.6 mL min^{-1} (measurements ECAL01 and ECAL03) are, respectively 0.8739, 0.8714 and 0.8677, indicating a minor decrease of sensitivity with increasing flow rate. In fact, the heat capacity of inflow liquid, entering at thermostat temperature, reduces the local temperature and, for instance, the output signal. The sensitivities for the TRIS reactions (TRIS01-0.2 mL min^{-1} and TRIS03-0.6 mL min^{-1}) are 0.9051 and 0.9039, respectively (based on the value of –47.44 kJ mol^{-1} for the protonation enthalpy [8]). Comparable to the electrical calibration, an increase of flow reduces the signal slightly. The TRIS-reaction based sensitivity is greater than the Joule-effect sensitivity. In fact, the heat in the electrical calibration heater is generated 'out of the cell' and, in TRIS reaction 'inside the cell' more close to the detectors.

A detailed analysis of the signals shows a periodic signal of approximately 0.1 μW peak to peak (Fig. 3). In the measurement marked TRIS03 the frequency is close to 0.25 Hz corresponding to periodic switching of a valve inside the pumps each 20 μL. For

Table 1 Values of the first time constant: experimental and simulated. *I*: signal ascent; *F*: signal decay i.e., established from the calorimeter output (curve) tail

Flows in mL min^{-1}	Joule effect (τ_1/s)		TRIS (τ_1/s)		Simulated (τ_1/s)
	I	*F*	*I*	*F*	
Stopped (0.0)	–	–	–	–	80.6
'slow' (0.2)	73.8	76.1	78.3	81.5	79.1
'medium' (0.4)	–	80.0	–	–	77.6
'fast' (0.6)	73.6	–	77.3	78.4	76.1

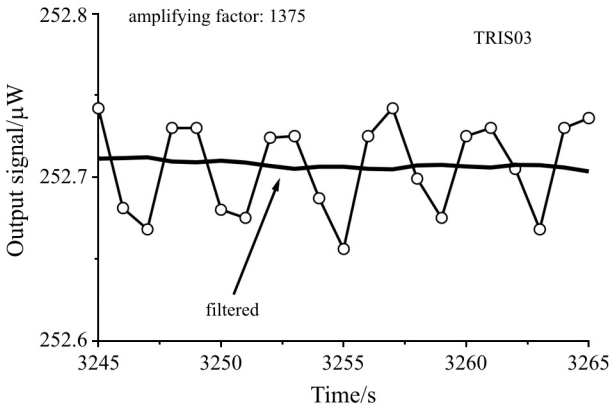

Fig. 3 Ripples in the output signal related with pump effects and filtered output for the TRIS03 measurement

each mixture the pump action induces some periodic perturbation with flow rate dependent frequency. From experimental analysis, the practical resolution is clearly better than 0.1 μW when, for instance, room temperature parasitic effects are completely avoided (Fig. 3). The pressure waves induced by piston pumps may enhance the mixture processes via an increased switching between the two flows. At the actual state of the art the subject requires further study.

The model

From an outline of the flow mixing cell and of the detector system (Fig. 4) a model with 36 elements is built. In the z-axis, a quarter of the system is decomposed in five shells with 7 heat capacities in each one). The global model includes an external heater (heat capacity 1) located in the fixed part of the calorimeter. According with the general scheme of the device, the cell includes the two inflow tubes inside the outflow tube with similar cross section for each one. In fact, the volume rate in the outflow tube is the sum of the inflow rates.

The model uses the classical RC-system with N heat capacities with thermal couplings between the elements. In the choice realized, the laboratory cell is divided into five shells of 10 mm thickness with 7 elements. Also, a separated heater for Joule-effect analysis in a fixed position in the bottom of the cell-container is considered. The general equation for a series of elements (heat capacities C_i in JK^{-1} and thermal couplings P_{ik} in WK^{-1} with an eventual contact with one thermostat at reference temperature (i.e., at T=0) reads,

$$W_i = C_i \frac{dT_i}{dT} + \sum_{k \neq i} P_{ik}(T_i - T_k) + P_{i0}T_i \qquad (1)$$

The mass transfer produces a transfer of heat power from j element to i element by,

$$W_i^* = g_{ij}(T_i - T_j) \qquad (2)$$

In a first approach the g_{ij} is proportional to density (ρ), heat capacity (c_p) and volume rate (f), i.e.,

$$g_{ij} = k\rho c_p f \qquad (3)$$

According to the model outlined in Fig. 4, the mass flow terms can be included in input and output flows; i.e., elements 3, 10, 17, 24 and 31 for inflow and 2, 9, 16, 23, and 30 for the output flow. When an excellent thermal contact is expected between input and output flows a mass-energy transfer can be included from element 30 to element 31.

An approach to parameter values

It is supposed that the tubes are made from Hastelloy that the main material of the cell is aluminum metal and that the used liquid is water. The basic thermal parameters used are given in Table 2 partially extracted from reference [9]. For instance, the heat capacity of element five (C_5) is obtained from the aluminum value and the volume of the element (133.52 mm^3). Also the couplings between elements 5 and 7 (P_{57}) and between 5 and surroundings (P_{50} bottom of the cell) are obtained by,

$$C_5 = \rho_{Al} c_{p\,Al} V_5 = 0.3377\ \mathrm{J\ K^{-1}} \qquad (4)$$

$$P_{57} = \frac{\dot{Q}_{57}}{T_5 - T_7} = A_{57} k_{Al} / \Delta x_{57} = 6.0044\ \mathrm{W\ K^{-1}} \qquad (5)$$

$$P_{50} = \frac{\dot{Q}_{50}}{T_5} = 250 A_{50} = 0.0055\ \mathrm{W\ K^{-1}} \qquad (6)$$

The A_{57} is the surface between the element 5 and 7, Δx_{57} is the distance between the representative points of the two elements and A_{50} is the surface of the element 5 in contact with still air.

Table 2 Basic thermal parameters of the used materials

Materials	Density/ kg m^{-3}	c_p/ J kg^{-1} K^{-1}	k/ W m^{-1} K^{-1}
Water	1000	4180	0.0607
Hastelloy [9]	9217	376.5	11.342
Aluminium	2700	936.7	209
Still air	P_{i0}&250* A (P_{i0} in W K^{-1} when A in m^2		

Static and dynamic effects

The model response (in model units or K) is analyzed for 'theoretical' dissipations in the elements 1 (Joule), 2, 9, 16, 23 and 30 in two cases. In the first one the inflow is realized at thermostat reference temperature (see Fig. 5). The second one (Fig. 5 right) uses a more effi-

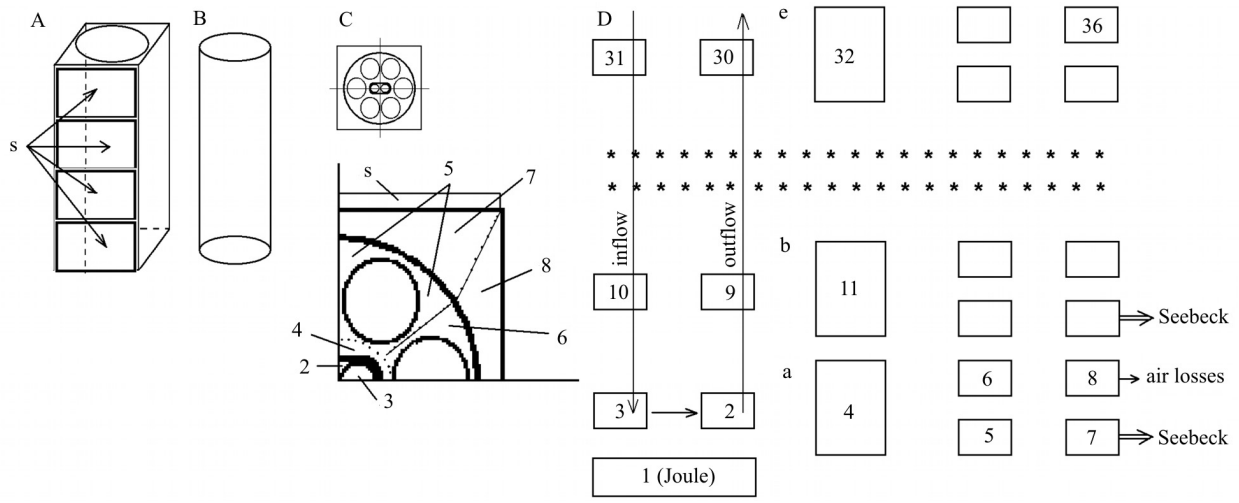

Fig. 4 Outline of the laboratory mixing chamber and neighbouring elements. A: block with 4 Seebeck plates (heat flow detectors) at each of the two opposite faces. B: mixing chamber (cylinder). C (top): outline of the chamber with the inner tube in the cell axis; the two input tubes and the residual space for the output. Bottom: schematic structure of the model based in a quarter of a shell of the chamber; 2: input tube, 3: output; 4: immediate vicinity; 5 and 6 elements related with the holes space; 7 and 8: elements associated to block contributions. D: schematic outline of the 36 heat capacities used in simulation

cient thermal coupling between inflow and outflow (mass-energy coupling between elements 31 and 30). Each analysis is realized for different simulated flows (0.0, 0.2, 0.4, and 0.6 mL min^{-1}). The Fig. 5 (left) shows the positional effects related to flow rate. An increase of flow rate reduces the sensitivity when the liquid enters at the external thermostat temperature. The flow rate cannot produce differences (Fig. 5 right) when an excellent coupling between outflow and inflow avoids the external temperature effect.

The figures clearly visualizes that the local sensitivity is practically constant inside the cell for the rough approach used in the model and, also, the reduced effect of flow rate when the inflow achieve the same temperature as the outflow. In other words, the minor local changes of sensitivity show the expected effects of increased heat losses in the top and bottom of the cell and, also, some flat sensitivity in the main central part of the cell. The experimental difference between Joule and chemical calibration can be explained by the difference between the origin of the heat production as shown in Fig. 5 (increase of sensitivity from Joule heater to other dissipation points at low flow rates). During Joule heating the heat is generated in the external heater and, eventually, cooled by the flow at thermostat temperature. In the chemical calibration experiment the heat is generated inside the mixing chamber and, also, moved with the liquid flow. This explains the higher sensitivity calculated from chemical calibration with the TRIS protonation reaction which is also a very fast process. The reaction is completed immediately after the mixing throttle and there is enough time for a complete heat exchange within the mixing chamber.

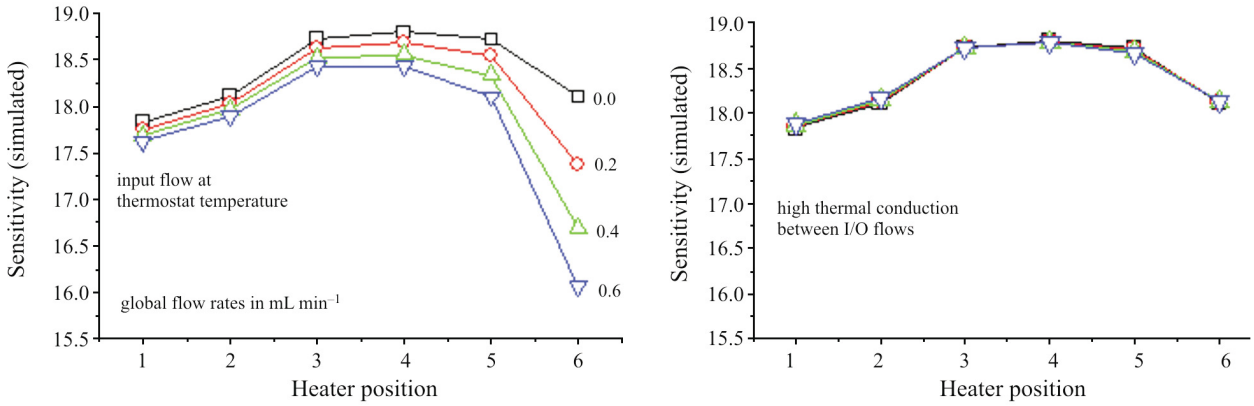

Fig. 5 Simulated results: plot of sensitivity *vs*. the position and the flow rates. The abscissa values 1, 2, 3, 4, 5 and 6 correspond to dissipation in the elements 1, 2, 9, 16, 23 and 30 (outflow elements), respectively. Left: input flow at thermostat temperature. Right: equal temperature in the inflow and outflow

Slow and fast reactions

Simulation permits local analysis with a larger choice of dissipations. In experimental analysis only Joule analysis in the heater and actual mixing measurements are possible. Independent dissipation in several elements is, from the experimental point of view, unavailable, i.e., Joule effects are only possible in the heater and only 'chemical reactions' dissipating simultaneously between the reaction chamber and the outflow tubing. If the reaction is completely realized inside or partially outside of the cell is a function of reaction rate and flow rate.

In order to analyze the expected effects according fast or slow reactions a first order dissipation mode is used. For instance the dissipation is constant for each position

$$W(t) = W_0 e^{-t/\tau} \quad (7)$$

For a constant flow, the flow displacement (z) and rate (v) are connected with time by $z=v\,t$ and the dissipation power can be formulated by,

$$W(z) = W_0 e^{-z/\lambda} \;\; with \;\; f = \nu A;\; \lambda = \nu\tau;\; \lambda = f\tau \,/\, A \quad (8)$$

The time constant is converted into λ, the characteristic reaction length. The available length (λ_{max}) in the cell is close to 50 mm (cell length).

For instance, the continuous curve is transformed into a step curve (using W_0=1) by integration over each element thickness:

$$W(z_1 \; to \; z_2)_{\text{mean value}} = e^{-z_1/\lambda} - e^{-z_2/\lambda} \quad (9)$$

Using the calculated values, the described model and the hypothesis that the flow enters at the thermostat temperature, the simulation delivers the sensitivity dependence on the time constant and flow rate (Table 3).

Figure 6 illustrates the output signals corresponding to three conditions marked by (*) in Table 3. The maximal steady state output is associated with a low λ value (under $0.33\lambda_{max}$). For intermediate values a small loss in energy is expected when part of the reaction is realized in the outflow tubing out of the cell. For values exceeding $0.50\lambda_{max}$ the detected energy decreases progressively. Hence, when the ratio λ/λ_{max} does not exceed 0.33 the chemical calibration is a satisfactory approach or the flow experiment delivers the correct reaction enthalpy. At the contrary, when the ratio overcomes 0.33 the percentage of energy loss increases and the reaction is too slow for the given experimental setup. However, this analysis relates only theoretical considerations based on simple reaction kinetics, heat and mass transport as well as complete and fast mixing. In fact, the real mixing process can proceed by diffusion between laminar flows (more slowly) or, eventually, by an accelerated mixing due to the geometrical particularities at the end of the inflow tubes or due to pressure waves caused by the pumps. The mixing process may benefit from combined effects of pressure waves but an adequate analysis requires further investigations.

Table 3 Effects of flow rate and reaction dynamics (time constant) on sensitivity. (*)output signal simulated in Fig. 6

Flow/ mL min^{-1}	Dissipation		Sensitivity/	Energy losses/%
	τ/s	λ/mm	in model units	
0.2	0.5	2.1	18.04	0.0
	2.0	8.3	18.16	0.2
0.4	0.5*	4.2	18.02	0.0
	2.0*	16.7	17.27	5.0
0.6	0.5	6.3	17.99	0.0
	2.0*	25	15.57	13.5

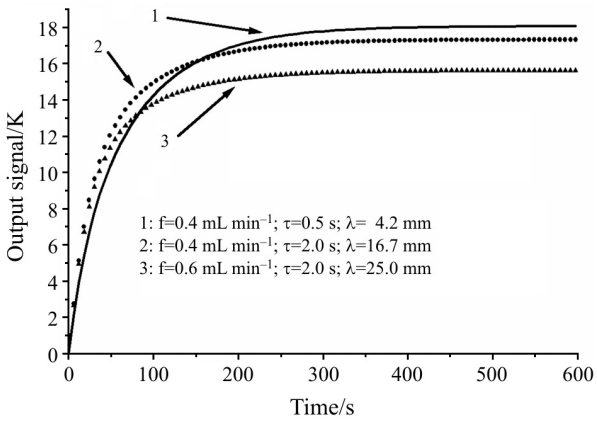

Fig. 6 Simulated output signals for several characteristic lengths. The signal level reduction in the steady state relates to energy losses

Conclusions

At the present state of the art the heat power resolution of the new TAM flow-mixing vessel seems to be better than 0.1 μW. The improved heat detector design together with the axial-symmetric position of the in/output tubes leads to reduced sensitivity changes inside the mixing cell. The sensitivity is, as expected, practically constant for heat generation inside the mixing chamber. The model suggests a minor reduction in the sensitivity for dissipations realized in the top part and in the bottom of the cell for increased heat losses to surroundings.

The mixing chamber with the outflow tube defines the appropriate length (or available volume for well detected heat of reaction). When the length ratio λ/λ_{max} exceed 0.33 the energy loss increases because a progressive part of the dissipated energy is generated out of the cell. In this case the reaction is too slow for the experimental setup. In fact, the mixing

can proceed by diffusion between laminar flows (extremely slowly) or, eventually, by accelerated mixing at the end of the inflow tubes activated by small pressure waves caused by the pumps. The understanding of these effects requires further investigation.

The established model shows similar behavior as the experimental measurements: a) higher sensitivity for fast chemical reactions in comparison to Joule-effect calibration, b) slight sensitivity reduction with increase of flow rate at thermostat temperature (the effect of the temperature in the inflow), c) shows the need of a preliminary analysis of the expected length (or volume) to ensure that the reaction is practically completed (and detected) inside the cell.

The complexity of the model can be increased in any way, i.e. by introducing explicitly the Seebeck elements, dividing the cell into more shells (in z-axis) and distinguishing between shells with and without holes…

Acknowledgements

This work was carried out and supported within the framework of an integrated action program between Spain (MEC: HA2003-0034) and Germany (DAAD: D/03/39344). RK acknowledges Thermometric AB for several remarks and information on the device behavior. VT also acknowledges the SOCRATES program for useful support. Helpful discussions with Dr. J. Lerchner are gratefully acknowledged.

References

1 F. Socorro, I de la Nuez and M. Rodríguez de Rivera, Measurement, 33 (2003) 241.
2 F. Socorro and M. R. de Rivera, J. Therm. Anal. Cal., 80 (2005) 763.
3 V. Torra, C. Auguet, J. Lerchner, P. Marinelli and H. Tachoire, J. Therm. Anal. Cal., 66 (2001) 255.
4 C. Auguet, F. Martorell, F. Moll and V. Torra, J. Therm. Anal. Cal., 70 (2002) 277.
5 C. Auguet, J. Lerchner, V. Torra and G. Wolf, J. Therm. Anal. Cal., 71 (2003) 407.
6 C. Auguet, J. Lerchner, P. Marinelli, F. Martorell, M. Rodriguez de Rivera, V. Torra and G. Wolf , J. Therm. Anal. Cal., 71 (2003) 951.
7 C. Auguet, J. L. Seguin, F. Martorell, F. Moll, V. Torra and J. Lerchner, J. Therm. Anal. Cal., In preparation
8 L. E. Briggner and I. Wadsö, J. Biochem. Biophys. Methods, 22 (1991) 101.
9 web page: www.hightempmetals.com/techdata/hitemphastbdata.php.

Received: July 27, 2005
In revised form: August 3, 2005

DOI: 10.1007/s10973-005-7148-z